Evidence of Fermi level control in a half-metallic Heusler compound Co_2MnSi by Al-doping: Comparison of measurements with first-principles calculations

Y. Sakuraba and K. Takanashi
Institute for Materials Research, Tohoku University, Katahira 2-1-1, Aoba-ku, Sendai 980-8577, Japan

Y. Kota, T. Kubota, M. Oogane, A. Sakuma, and Y. Ando
Department of Applied Physics, Graduate School of Engineering, Tohoku University, Aoba-yama 6-6-05, Aramaki, Aoba-ku, Sendai 980-8579, Japan

(Received 4 March 2010; published 22 April 2010)

The Fermi level (E_F) control of half-metallic Heusler alloy Co_2MnSi by Al-doping was challenged in magnetic tunnel junctions with a $Co_2MnAl_xSi_{1-x}$ (CMAS) electrode. The observed bias voltage dependence on tunneling conductance (G-V curves) clearly shows a shift in E_F toward the center of the half-metallic gap with x, which showed excellent agreement with our first-principles calculations. However, the ratio of tunnel magnetoresistance (TMR) at 10 K to that at room temperature does not exhibit a remarkable change with x. The weak exchange energy at the CMAS interface may be the origin for the large temperature dependence of the TMR ratio.

DOI: 10.1103/PhysRevB.81.144422 PACS number(s): 75.47.−m, 71.55.Ak, 75.50.Cc

I. INTRODUCTION

Certain Co-based Heusler alloy compounds, such as Co_2MnSi (CMS), are promising in the realization of the high spin-polarized state of conduction electron at room temperature (RT) due to their half-metallic band structure and high Curie temperatures.[1,2] The high spin polarization of these compounds has been evidenced experimentally by recent extensive studies on tunnel magnetoresistance (TMR) (Refs. 3–8) and current-perpendicular-to-plane giant magnetoresistance (CPP-GMR) effects.[9–12] Our previous studies on epitaxially grown CMS-based magnetic tunnel junctions (MTJs) have shown a giant TMR ratio of 570% at 2 K for the CMS/Al-O/CMS structure, clearly indicating the half-metallic nature of CMS at least at low temperature (LT). Because the biggest drawback of half-metallic Heusler alloys is the relatively small half-metallic energy gap (less than 1 eV), the position of E_F in the half-metallic gap is an important factor for determining the stability of half-metallicity against temperature. Additionally, the half-metallic energy gap of CMS has been observed in the applied bias voltage dependence of differential tunneling conductance ($G-V$).[13,14] The observed tiny energy separation between E_F and the conduction band (CB), which is less than 10 meV, was suggested as a plausible origin for the rapidly decreasing TMR ratio with temperature and the disappearance of half-metallicity at RT because the thermal fluctuation at RT of about 30 meV causes a large depolarization effect due to smearing of electronic structure. Thus, one solution to improve the endurance of half-metallicity against thermal fluctuation is to control E_F in CMS by the optimum replacement of Si by Al. Because Al has one less valence electron than Si, substitution should help control the position of E_F to the center of the half-metallic gap. Although numerous studies have examined E_F control by impurity doping in semiconductor-based systems, few have examined E_F control by impurity doping in metal-based systems[15,16] especially in half-metals, despite their importance. Recently, Shan *et al.* reported a large TMR ratio of 102% at RT in the $Co_2FeAl_{0.5}Si_{0.5}$-based MTJ and claimed the demonstration of half-metallicity at RT by Fermi level tuning according to the simple fitting of TMR vs the T curve based on the spin-wave excitation model.[15] In that study, however, no direct evidence for the tuning of Fermi level was obtained because of no systematic change in Al/Si composition and no comparison with theoretical investigation. The purpose of the present study is to fabricate MTJs with an epitaxial $Co_2MnAl_xSi_{1-x}$ electrode having different Al concentrations x and to systematically investigate TMR and $G-V$ behavior as a function of x. Theoretical investigations about the electronic structure of CMAS were also carried out based on first principles for a systematic comparison with the experimental results.

Figure 1 shows the calculated spin-resolved DOS for $B2$-structured $Co_2MnAl_xSi_{1-x}$ (CMAS) with different Al concentrations (x). The tight-binding linear muffin-tin orbital method within the framework of the local spin density func-

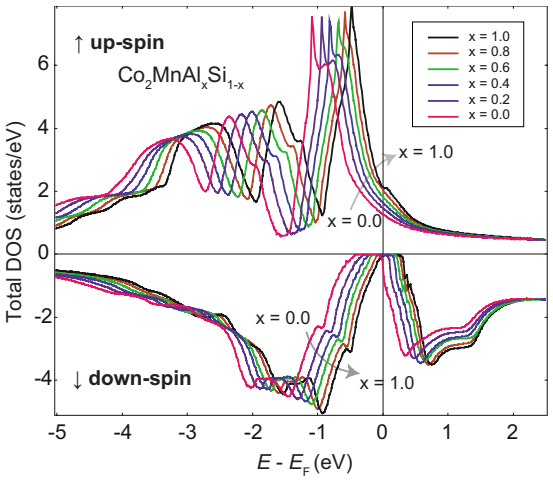

FIG. 1. (Color online) Spin-resolved density of states (DOS) for $Co_2MnAl_xSi_{1-x}$ (x=0.0, 0.2, 0.4, 0.8, and 1.0) in the $B2$ structure by first-principles calculations.

tional theory was used in the band calculation.[17,18] The partial disorder in the $B2$ structure was treated by the coherent potential approximation using the Green's function technique. The lattice constants for Co_2MnSi and Co_2MnAl were 5.655 Å and 5.755 Å, respectively, and the value estimated from Vegard's law was used for each CMAS (x=0.2, 0.4, 0.6, and 0.8). Increasing x shifted the position of E_F toward the VB without a loss in the half-metallic gap structure.

II. SAMPLE PREPARATION AND EXPERIMENTAL METHOD

All the samples were fabricated on a Cr-buffered MgO (001) single-crystalline substrate using an UHV-compatible magnetron sputtering system. $Co_2MnAl_xSi_{1-x}$ epitaxial bottom electrodes with different x concentrations were prepared by a cosputtering technique using $Co_{43.7}Mn_{27.95}Si_{28.35}$ and $Co_{43.7}Mn_{27.95}Al_{28.35}$ sputtering targets. The Al concentration x was controlled in the range from 0 to 1 by adjusting the input power of each sputtering target while maintaining a constant total deposition rate of 0.032 nm/s. The postannealing temperature for the CMAS electrode was fixed at 773 K for all samples. The stacking structure of MTJ was MgO-subs/Cr(40 nm)/CMAS(30)/Mg(0.8)/Al(1.0)-O/$Co_{75}Fe_{25}$(5)/$Ir_{22}Mn_{78}$(10)/Ta(5). A thin Mg layer inserted between the CMAS and the Al-O barrier efficiently prevented magnetic contaminants from forming at the CMAS surface due to its small formation enthalpy of oxides as demonstrated in previous papers.[19,20] Note that, transmission electron microscopy image observation found that tunneling barrier in our samples is basically amorphous not crystallized epitaxially like that in Ref. 15; thus, enhancement of spin polarization by coherent tunneling can be excluded. The chemical composition, crystal structure, and surface flatness in the CMAS electrode were characterized by scanning electron microscopy with energy dispersive x-ray analysis (SEM/EDX), x-ray diffraction (XRD), and atomic force microscopy (AFM), respectively. Magnetoresistance (MR) measurements were performed using the standard dc four-probe method, while the G-V curves were measured at 10 K using an ac lock-in amplifier technique. The bias voltage was defined as positive when electrons tunnel from the upper $Co_{75}Fe_{25}$ to the lower CMAS electrode.

III. EXPERIMENTAL RESULT

The Al concentration in each CMAS electrode analyzed by SEM/EDS (x_{EDX}) agreed well with the nominal Al concentration (x) as shown in Fig. 2. For simplicity, herein the value of x is used in the notation of each sample. All samples displayed the (002) superlattice peak reflecting the $B2$ structure without a pronounced intensity change with x in XRD patterns. The calculated intensity ratio of the (002) superlattice peak to the (004) fundamental peak in all samples exhibited nearly perfect $B2$ ordering. The out-of-plane and in-plane XRD measurements did not show detectable peaks of the $L2_1$ structure for all x. As shown in Fig. 2, the lattice constant of CMAS estimated from the (002) peak followed Vegard's law for x between 0.0 and 0.2 indicating that Al

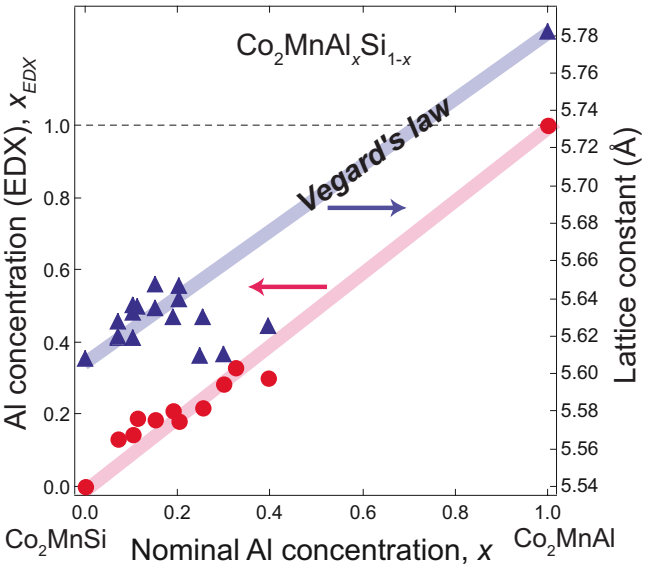

FIG. 2. (Color online) Nominal Al concentration dependence of the actual Al concentration observed by SEM/EDX (left) and lattice constant for CMAS estimated from the (004) peak in the XRD patterns (right).

atoms were substituted into the Si sites without phase separation. The AFM observation confirmed that all the CMAS electrodes had flat surface morphologies with an average roughness less than 0.3 nm indicating no remarkable effect of interface roughness on TMR properties in all MTJs with different x.

Figures 3(a) and 3(b) show the experimental G-V curves for the CMAS/(Mg/Al)-O/CoFe-MTJs at 10 K and the calculated down-spin DOS in the CMAS around E_F, respectively. The G-V curves were measured in the parallel configuration. As illustrated in Fig. 4, if the E_F lies in the half-metallic energy gap in CMAS and considering only elastic tunneling, the edge of valence (conduction) band is observed in the parallel state when the applied bias voltage V reaches—δ_{VB}/e (δ_{CB}/e), where δ_{VB} (δ_{CB}) denotes the energy difference between E_F and the edge of VB (CB). In Fig. 3(a), the V, where tunnel conductance (G) began to increase (here defined as V_n), clearly shifted toward zero with x monotonically, and the shape of each curve is similar to those of the calculated DOS in Fig. 3(b). Figure 5 shows the x dependence of the observed eV_n and calculated δ_{VB}, which both were estimated using a second derivative numerically for each curve. eV_n agreed well with δ_{VB} indicating successful control of E_F in the half-metallic energy gap by Al-doping to CMS. However, in the positive V region, G rapidly increased below a very small V less than +10 mV for all samples and the G-V did not remarkably change with x. Thus, unlike the monotonic increase of the δ_{CB} with x as shown in Fig. 5, V where G begins to increase (defined as V_p) does not vary with x in the positive V region.

IV. DISCUSSION

There are two possible explanations for the small eV_p for all x. First is the nonquasiparticle (NQP) states appearing just

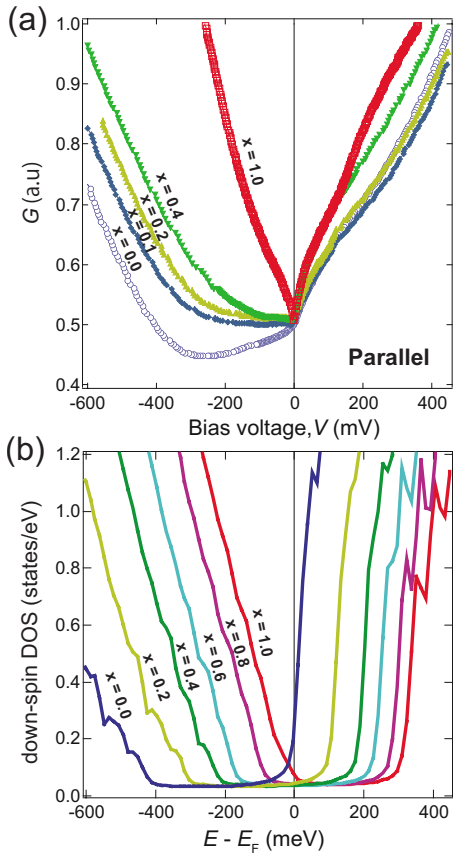

FIG. 3. (Color online) (a) Bias voltage dependence of tunneling conductance in $Co_2MnAl_xSi_{1-x}$‖CoFe-MTJs with different x at 10 K and (b) calculated total DOS in the down-spin channel for $Co_2MnAl_xSi_{1-x}$ around E_F.

above E_F, which were predicted by the LSDA (local spin density approximation) +DMFT (dynamical mean field theory) approach, where the electron-correlation effects are treated within the framework of DMFT.[21,22] Liviu *et al.* recently applied DMFT to the band structure of CMS and found the existence of NQP states just above E_F in the half-metallic band gap.[23] Therefore, the observed tiny eV_p may reflect the NQP states just above E_F in CMAS. However, the validity of applying DMFT to Heusler alloy systems remains

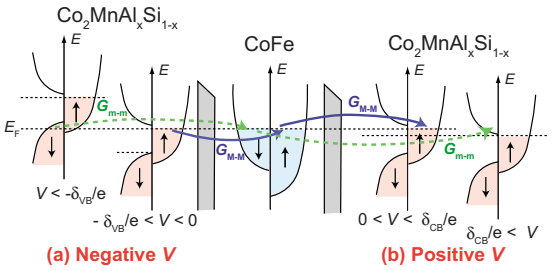

FIG. 4. (Color online) Schematic diagram of the elastic tunneling process in CMAS‖CoFe-MTJ in the parallel configuration for (a) negative V and (b) positive V. When the bias voltage V is between $-\delta_{VB}/e$ and δ_{CB}/e, electron tunneling occurs only from majority to majority ($G_{M\text{-}M}$), but once V is below $-\delta_{VB}/e$ (above δ_{CB}/e), a new tunneling from $G_{m\text{-}m}$ from the VB (to the CB) of the half-metallic gap arises.

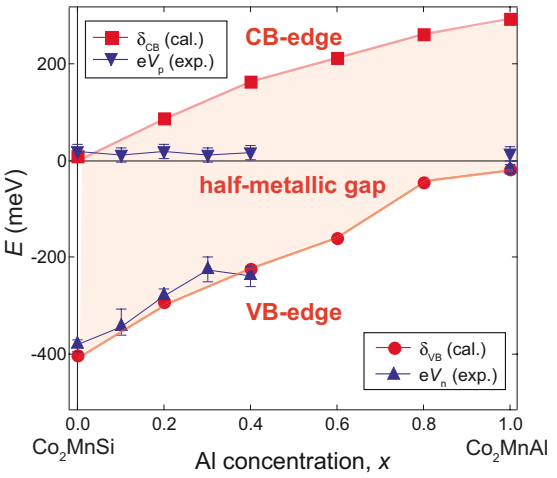

FIG. 5. (Color online) Al concentration dependence of the calculated energy separation between the edges of the VB, CB, E_F (δ_{VB}, δ_{CB}), and the observed eV_n and eV_p in the G-V curves.

controversial due to insufficient information about the electron-correlation effect in Heusler alloys. Additionally, a recent experiment using photoelectron spectroscopy did not find a remarkable temperature dependence of the VB spectrum in CMS, which is inconsistent with the prediction based on DMFT.[24] The second more possible origin for the small eV_p is inelastic tunneling processes involving spin-flipping at the CMAS surface. For the half-metal based MTJs, Mavropoulos *et al.* theoretically noted the creation of interface states at E_F within the half-metallic gap of the half-metal/barrier interface and the spin-flipping process through the interface states mediated by magnon excitation.[25] When we consider the ideal half-metallic state in the bulk region, these interface states do not work as emitters of a tunneling electron, but can work as collectors of tunneling electrons and contribute to the tunnel conductance, G, through a spin-flipping process at the electron-received interface (see Fig. 6).[26] Based on this prediction, a down-spin electron is emitted from CoFe in the positive V region and collected by the interface states at CMAS. The electron then flows into the up-spin states in the bulk region by a spin-flipping process. Although our recent experiments using Brillouin light scattering spectroscopy have revealed a large exchange stiffness in CMAS epitaxial films,[27] Sakuma *et al.* recently reported a remarkable reduction in the exchange energy of Co atoms at the barrier interface in their first-principles calculations for CMS/MgO and CMA/MgO bilayer systems.[28] Therefore, it is hypothesized that such local weakening of the exchange energy at the barrier interface is responsible for a number of low energy magnon excitations by hot electrons with energy less than a few tens of meV. Thus, the no shift of the V_p with x in the G-V curves may be due to the dominant contribution of inelastic tunneling in the positive bias region.

Figure 7 summarizes the x dependence of TMR at RT and 10 K in the CMAS/(Mg/Al)-O/CoFe-MTJs. CMS-MTJ (x =0.0) showed a TMR of 87% at RT and 194% at 10 K, which give spin polarizations of 0.61 and 0.98, respectively, for CMS from Julliere's equation (assuming 0.50 for the CoFe).[29] The TMR at RT and 10 K monotonically decreased

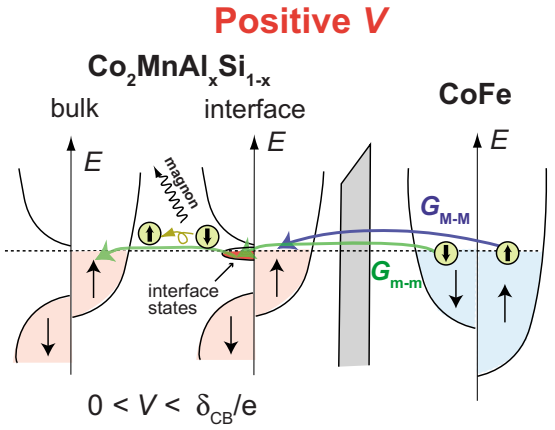

FIG. 6. (Color online) Schematic diagram of the plausible inelastic tunneling process in CMAS‖CoFe-MTJ in the parallel configuration for positive V. Even when bias voltage V is below δ_{CB}/e, electron tunneling occurs from minority to minority ($G_{m\text{-}m}$) mediated by interfacial in-gap states appeared in CMAS. Tunneling minority-spin electron from CoFe flips its spin at the CMAS interface with a magnon excitation and then goes into majority-spin states in CMAS bulk region.

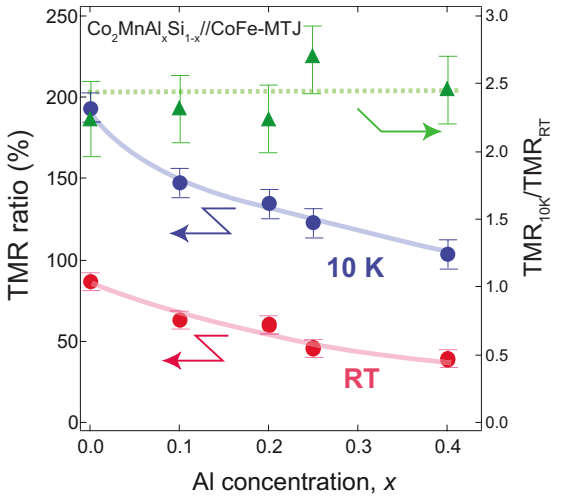

FIG. 7. (Color online) Al concentration dependence of the TMR ratio (left axis) and the ratio of TMR ($T=10$ K) to TMR (RT) (right axis) in CMAS‖CoFe-MTJs.

to 43% and 103%, respectively, as the x up to 0.4, which may be caused by creating a small amount of contamination at the CMAS/(Mg/Al)-O interface with increasing Al/Si ratio. Interestingly, the ratio of TMR at 10 K to that at RT, i.e., $TMR_{10\ K}/TMR_{RT}$ showed a large value of almost 2.3–2.6 for all x from 0 to 0.4 implying that the position of E_F does not dominantly contribute to the large temperature dependence of TMR in CMAS-based MTJs. Therefore, the weak exchange energy at the CMAS interface should explain the large temperature dependence of the TMR ratio and the rapid increase of G with a small positive excitation voltage in the G-V curves [Fig. 3(a)] compatibly in all x regions.

V. SUMMARY

In conclusion, in this study TMR and G-V behavior were systematically investigated for MTJs with an epitaxial $Co_2MnAl_xSi_{1-x}$ electrode for different x. Controlling of E_F toward the center of the half-metallic gap by Al-doping to CMS was clearly demonstrated in the bias voltage dependence of tunneling conductance (G-V) and evidenced by confirming the consistency with our first-principles calculations. Nevertheless, the ratio of TMR at 10 K to that at RT did not change with the Al concentration. The weak exchange energy at the CMAS/barrier interface, which is speculated from the rapid increase of G at a small positive bias voltage in the G-V curves, is responsible for the large temperature dependence of TMR.

ACKNOWLEDGMENTS

This work was supported by a Grant-in-Aid for Scientific Research in Priority Area "Creation and control of spin current" (Grant No. 19048004) and Young Scientists (B) (Grant No. 20760005) from MEXT, Japan and partially supported by the Strategic Japanese-German Cooperative Program on "Nanoelectronics."

[1] S. Ishida, S. Fujii, S. Kashiwagi, and S. Asano, J. Phys. Soc. Jpn. **64**, 2152 (1995).
[2] S. Picozzi, A. Continenza, and A. J. Freeman, Phys. Rev. B **66**, 094421 (2002).
[3] Y. Sakuraba, J. Nakata, M. Oogane, H. Kubota, Y. Ando, A. Sakuma, and T. Miyazaki, Jpn. J. Appl. Phys., Part 2 **44**, L1100 (2005).
[4] Y. Sakuraba, M. Hattori, M. Oogane, H. Kubota, Y. Ando, H. Kato, A. Sakuma, and T. Miyazaki, Appl. Phys. Lett. **88**, 192508 (2006).
[5] S. Tsunegi, Y. Sakuraba, M. Oogane, K. Takanashi, and Y. Ando, Appl. Phys. Lett. **93**, 112506 (2008).
[6] T. Ishikawa, T. Marukame, H. Kijima, K.-I. Matsuda, T. Uemura, M. Arita, and M. Yamamoto, Appl. Phys. Lett. **89**, 192505 (2006).
[7] T. Taira, T. Ishikawa, N. Itabashi, K.-I. Matsuda, T. Uemura, and M. Yamamoto, J. Phys. D **42**, 084015 (2009).
[8] N. Tezuka, N. Ikeda, F. Mitsuhashi, and S. Sugimoto, Appl. Phys. Lett. **94**, 162504 (2009).
[9] K. Yakushiji, K. Saito, S. Mitani, K. Takanashi, Y. K. Takahashi, and K. Hono, Appl. Phys. Lett. **88**, 222504 (2006).
[10] T. Furubayashi, K. Kodama, H. Sukegawa, Y. K. Takahashi, K. Inomata, and K. Hono, Appl. Phys. Lett. **93**, 122507 (2008).
[11] Y. Sakuraba, T. Iwase, K. Saito, S. Mitani, and K. Takanashi, Appl. Phys. Lett. **94**, 012511 (2009).
[12] T. Iwase, Y. Sakuraba, S. Bosu, K. Saito, S. Mitani, and K. Takanashi, Appl. Phys. Express **2**, 063003 (2009).
[13] Y. Sakuraba, T. Miyakoshi, M. Oogane, H. Kubota, Y. Ando, A.

Sakuma, and T. Miyazaki, Appl. Phys. Lett. **89**, 052508 (2006).
[14] Y. Sakuraba, M. Hattori, M. Oogane, H. Kubota, Y. Ando, A. Sakuma, and T. Miyazaki, J. Phys. D **40**, 1221 (2007).
[15] R. Shan, H. Sukegawa, W. H. Wang, M. Kodzuka, T. Furubayashi, T. Ohkubo, S. Mitani, K. Inomata, and K. Hono, Phys. Rev. Lett. **102**, 246601 (2009).
[16] B. Balke, G. H. Fecher, H. C. Kandpal, C. Felser, K. Kobayashi, E. Ikenaga, J. J. Kim, and S. Ueda, Phys. Rev. B **74**, 104405 (2006).
[17] O. K. Andersen, Phys. Rev. B **12**, 3060 (1975).
[18] J. Kudrnovský and V. Drchal, Phys. Rev. B **41**, 7515 (1990).
[19] N. D. Telling, P. S. Keatley, G. van der Laan, R. J. Hicken, E. Arenholz, Y. Sakuraba, M. Oogane, Y. Ando, and T. Miyazaki, Phys. Rev. B **74**, 224439 (2006).
[20] Y. Sakuraba, M. Hattori, M. Oogane, H. Kubota, Y. Ando, A. Sakuma, N. D. Telling, P. Keatley, G. van der Laan, E. Arenholz, R. J. Hicken, and T. Miyazaki, J. Magn. Soc. Jpn. **31**, 338 (2007).
[21] L. Chioncel, E. Arrigoni, M. I. Katsnelson, and A. I. Lichtenstein, Phys. Rev. Lett. **96**, 137203 (2006).
[22] V. I. Anisimov, A. I. Poteryaev, M. A. Korotin, A. O. Anokhin, and G. Kotliar, J. Phys.: Condens. Matter **9**, 7359 (1997).
[23] L. Chioncel, Y. Sakuraba, E. Arrigoni, M. I. Katsnelson, M. Oogane, Y. Ando, T. Miyazaki, E. Burzo, and A. I. Lichtenstein, Phys. Rev. Lett. **100**, 086402 (2008).
[24] K. Miyamoto, A. Kimura, Y. Miura, M. Shirai, M. Ye, Y. Cui, K. Shimada, H. Namatame, M. Taniguchi, Y. Takeda, Y. Saitoh, E. Ikenaga, S. Ueda, K. Kobayashi, and T. Kanomata, Phys. Rev. B **79**, 100405(R) (2009).
[25] P. Mavropoulos, M. Ležaić, and S. Blügel, Phys. Rev. B **72**, 174428 (2005).
[26] T. Ishikawa, N. Itabashi, T. Taira, K.-I. Matsuda, T. Uemura, M. Arita, and M. Yamamoto, Appl. Phys. Lett. **94**, 092503 (2009).
[27] T. Kubota, J. Hamrle, Y. Sakuraba, O. Gaier, M. Oogane, A. Sakuma, B. Hillebrands, K. Takanashi, and Y. Ando, J. Appl. Phys. **106**, 113907 (2009).
[28] A. Sakuma, Y. Toga, and H. Tsuchiura, J. Appl. Phys. **105**, 07C910 (2009).
[29] M. Julliere, Phys. Lett. **54A**, 225 (1975).